



Size- and temperature-dependent oxidative pyrolysis and auto-ignition of spherical beech and spruce wood

Christoph Preimesberger^{1,2} · Maximilian Wondrak² · Axel Solt-Rindler^{1,2} · Christoph Pfeifer³ · Christian Hansmann^{1,2}

Received: 26 September 2022 / Revised: 14 February 2023 / Accepted: 16 February 2023
© The Author(s) 2023

Abstract

Opposed to piloted ignition, where a substance is ignited by an external flame or spark, the term auto-ignition describes the onset of combustion by spontaneous ignition without an external source. In this study, the influence of the size of spherical wood samples and the temperature surrounding the samples was investigated by performing ignition experiments in a muffle furnace with beech and spruce wood. On a specially constructed rig, spheres with four different diameters (8 mm, 12 mm, 18 mm, and 25 mm) were put into a preheated furnace at five isothermal temperatures (240 °C, 270 °C, 300 °C, 330 °C, and 360 °C). For every temperature, diameter, and wood species, the experiments were repeated eight times, and positions of the spheres on the rig were changed for every measurement. Temperatures inside the samples were recorded with thermocouples (TC) positioned in holes drilled to the middle of the spheres. With rising size and temperature, samples were more prone to auto-ignition in a glowing mode, due to a larger, highly reactive pyrolyzed surface and internal overheating. During heating and oxidative pyrolysis, isothermal phases were present at approximately 360 °C in the recorded temperature curves. The comparison to simultaneous thermal analysis (STA) measurements shows decomposition of hemicelluloses, and cellulose is highest around 360 °C. It is concluded that pyrolysis and disintegration of the main wood constituents use up all arising energy. Due to differences in the composition of the wood polymers, beech wood samples already ignite at lower temperatures compared to spruce wood samples with the same diameter. It can be concluded that the size is a critical factor for auto-ignition at the used temperatures. Larger samples will produce more volatile compounds during pyrolysis and have a larger pyrolyzed, porous surface area where heterogeneous oxidation reactions can happen. The influence of the size is already critical at differences on the millimetre scale.

Keywords Auto-ignition · Oxidative pyrolysis · Size dependence · Temperature dependence · Solid wood

1 Introduction

Auto-ignition describes the process of ignition without the influence of a spark or a flame [1]. It can either take place in the gas phase or directly on the surface. For the auto-ignition of gases, the lower flammability limit of volatiles and a sufficiently high temperature must be reached to trigger homogeneous reactions between pyrolysis products and oxygen [2]. On the porous surface of the material, heterogeneous reactions between oxygen and carbon in combination with internal self-heating can induce a combustion process [3, 4]. Temperatures at which auto-ignition was observed depend largely on the devices used and the sample geometry. The lowest recorded temperatures for heterogeneous auto-ignition of wood are in the range of 240 °C [5]. Due to its multi-step decomposition, which produces highly reactive

✉ Christoph Preimesberger
christoph.preimesberger@boku.ac.at;
c.preimesberger@wood-kplus.at

¹ Wood K plus - Competence Center for Wood Composites & Wood Chemistry, Kompetenzzentrum Holz GmbH, Altenberger Straße 69, A-4040 Linz, Austria

² Department of Material Sciences and Process Engineering, Institute of Wood Technology and Renewable Materials, University of Natural Resources and Life Science (BOKU), Konrad Lorenz-Straße 24, A-3430 Tulln an der Donau, Austria

³ Department of Material Sciences and Process Engineering, Institute of Chemical and Energy Engineering, University of Natural Resources and Life Science (BOKU), Muthgasse 107/I, A-1190 Vienna, Austria

charcoal not only under non-oxidative but also under oxidative conditions, especially at lower heating rates, wood is one of the few materials that exhibit this kind of phenomenon [6, 7]. Other names for the described process are oxidative pyrolysis or, at temperatures of approx. 180 to 240 °C, torrefaction [8, 9]. Pyrolysis describes the heating and subsequent thermal decomposition of a material without the influence of an oxidising agent. While heating up wood or biomass, pyrolysis also happens in an oxidising atmosphere, as gaseous pyrolysis products streaming away from the material prohibit the contact of oxygen rich air with the surface, building up an oxygen-free diffusion zone [10]. When devolatilization is complete, the flow of volatiles ends and atmospheric oxygen can come into contact with the hot charcoal. On the porous charcoal, with a high internal surface, chemisorption of oxygen and direct oxidation of carbon to carbon monoxide and carbon dioxide can initiate a glowing or smouldering combustion process [11–13]. Transition from smouldering and glowing combustion to flaming and the other way around is possible and poses a major safety concern [14]. Current studies mostly focus on size differences at centimetre to metre scales or use a kinetic approach to the topic through microscale measurements (e.g. thermal analysis) and attempt to simulate the behaviour of wood on a larger scale [15, 16]. But biomass, including solid wood, usually exhibits a lot of physical and chemical variations, which are hard to implement in models and simulations, but influence pyrolysis, ignition, and combustion on all scales [17–19]. Therefore, experiments are needed to show the range of possible outcomes.

Many authors describe the influence of the size and geometry of wood on the auto-ignition temperature, and this is often done in the form of either small wood particles in bulk [20] or wood-based materials, with homogenous density profiles (e.g. pellets) [21, 22]. This has the huge advantage that different shapes and large homogeneous volumes can be produced by filling the baskets with the material, which is impossible with solid wood, as its properties change with the dimension and cutting direction [23]. The results of these experiments can be analysed and interpreted using the Frank-Kamenetskii theory (FK analysis), calculating the kinetic constants and extrapolating the ignition temperature of small basket experiments (cm range) to bigger sizes [20, 24]. Auto-ignition studies on solid wood or wood-based materials usually apply heating just from one side on a flat surface [3, 25]. The cone calorimeter is a device specially constructed for ignition studies on various materials but does not show the influence of the volume of a body as well. For calculations of safety aspects in the built environment, this is usually sufficient, since in most cases the impact of heat and fire is on a plain surface [24].

But the oxidative pyrolysis, self-heating, and auto-ignition of wood particles of all sizes depend on many aspects,

above all the surface area and the surface to volume ratio [26]. Influences of the volume and the conditions at pyrolysis (e.g. heating rate and maximum temperature) are well-known for particles in the range of micrometres (e.g. TGA) and in bulk (e.g. FK-Analysis), but only few studies look at solid wood in the range of centimetres [20, 27, 28]. Daouk et al. used a makro-TG to study the influence of oxygen concentration on temperatures arising during pyrolysis at temperatures of 400 to 600 °C isothermally and under dynamic heating to 800 °C [6, 29]. Additionally, the wood species and the chemical composition have an influence on the pyrolysis and oxidation reactions taking place [17, 30, 31].

In the present work, the influences of small size variations of spherical solid wood samples and the wood species on the auto-ignition properties are analysed. Wood or its decomposition products can already ignite at furnace temperatures of 240 °C or below, so the experiments focus on the range from 240 to 360 °C. The temperature range chosen for the present study represents a less investigated temperature range because it is too low for pyrolysis or gasification experiments and the time period studied is too high for torrefaction. With the results, fundamental insights into the degasification and ignition behaviour of wood shall be gained. What happens in the stated temperature range with different wood species is relevant for an efficient and safe use of wood and wood-based products in the near future. On the one hand, these fundamental findings will improve safety aspects in wooden buildings, as a secure, knowledge-based design can be adapted for different wood species not yet used in construction, and on the other hand, the new findings can improve the efficiency of thermo-chemical conversion processes.

2 Materials and methods

2.1 Auto-ignition experiments

Samples made from solid beech (*Fagus sylvatica*) and spruce (*Picea abies*) with four different diameters (8 mm, 12 mm, 18 mm, and 25 mm) were bought for the experiments. Samples were selected with similar growth ring deviations to get material that had very low variability in its properties. However, due to the nature of solid wood, the spheres used are not completely homogeneous in their properties. A spherical geometry was chosen, because it has no corner or edges, where the surface to volume ratio is lower. Differences in the density between the four dimensions can be seen in Fig. 1. These differences appear because of different ratios of early to late wood, which are more pronounced in angiosperms like spruce and are more present in smaller samples. Beech as a diffuse porous tree species is less prone to these differences [18]. Density was measured by weighing and

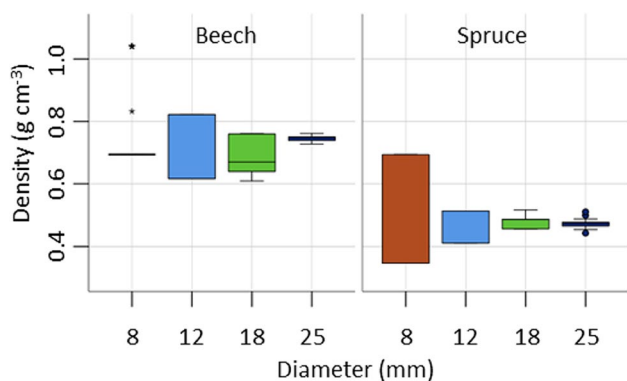


Fig. 1 Density of beech and spruce spheres with five different diameters ($n = 40$)

measuring the diameter directly before the experiment. The density is given at a moisture content of approx. 7%, which was measured by the oven dry method on spheres that were stored in the laboratory with the samples for the ignition experiments. These spheres were intentionally not pre-dried, as this experiment should show the auto-ignition properties of material stored at room climate. The overall mean density of beech and spruce is 0.73 g cm^{-3} and 0.43 g cm^{-3} , respectively. There are no significant differences between the spruce samples (ANOVA with $\alpha = 0.95$), but a post-hoc Scheffé test shows that significant differences are present between the 18 mm and the rest of the beech samples. Fuel properties (proximate and ultimate analysis), calorific value, and the chemical composition (taken from [32]) for the used wood species are shown in Table 1.

Holes with a diameter of 1.5 mm were drilled in each specimen through the central growth ring along the longitudinal axis (see drawing Fig. 2), to fix thermocouples (TC) (type K, non-shielded junction) in the middle. Thermocouples were connected to a PCE-T390 datalogger. Temperatures in the samples and the surrounding furnace were recorded every second. Experiments were performed in a muffle furnace (Carbolite AAF 1100) at five consecutive temperature levels between 240 and 360 °C with increments of 30 °C. The spheres were fixated on a specially constructed rig (see Fig. 2), equipped with the thermocouples and then placed in the preheated oven. The experiments lasted for a maximum duration of 2 h. At every temperature level eight repetitions, with randomised sample positions were carried out, an example of the sphere arrangement is shown in Fig. 2. The distance between the individual spheres was at least equal to the diameter of the largest sphere to minimise interactions between the reacting samples; additionally, the switching of the positions should homogenise the results. Care is taken to ensure identical positioning of the samples to minimise effects generated by the anisotropy of the

Table 1 Proximate analysis, calorific value, ultimate analysis, and the chemical composition of solid beech and spruce wood

	Proximate analysis (wt. % d.b.)				Chemical composition (wt.%) ^b									
	Fixed carbon	Ash	Volatile matter	Calorific value kJ/kg	C	H	N	O ^a	Cellulose	Glucomannan	Glucuronoxylan	Other poly-saccharides	Lignin	Extractives
Beech	12.9	0.4	81.9	18339.0	48.6	6.1	0.2	45.1	39.4	1.3	27.8	4.2	24.8	1.2
Spruce	12.4	0.3	82.1	18704.5	48.9	6.3	0.4	44.4	41.7	16.3	8.6	3.4	27.5	1.7

^aBy difference

^bFrom Sjöström [32]

Fig. 2 Picture of the experimental setup and a drawing of the positioning of the spheres on the rack

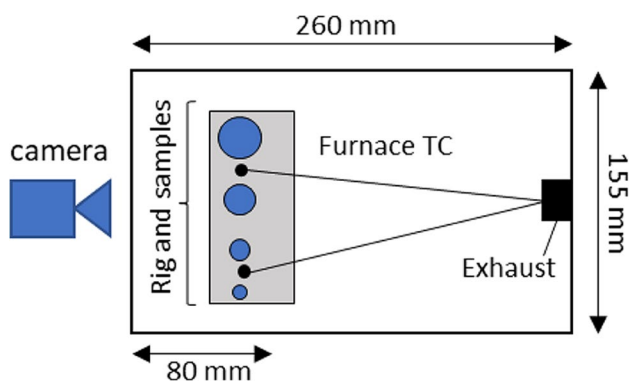


Fig. 3 Drawing of the mode of ignition experiment setup

wood, and spheres are positioned along the longitudinal axis of the samples, as seen in Fig. 2. For every experiment, the rig was positioned 80 mm inside the furnace. To investigate whether flaming or glowing ignition is happening, experiments with the original muffle furnace door switched out for a glass window were conducted. A drawing of the setup for the mode of ignition experiments is shown in Fig. 3. At each temperature level, a set of 4 spheres with the already mentioned diameters were put into the muffle furnace and heated at isothermal temperatures. The oxidative pyrolysis and possible subsequent combustion taking place inside the furnace chamber were recorded with a video camera. As shown in Fig. 3, thermocouples are positioned between the 25- and 18-mm spheres and the 12- and 8-mm spheres, which recorded the furnace temperatures and possible arising temperatures and heat emissions from the ignition of the spheres. Mode of ignition experiments were performed at 270 °C, 300 °C, 330 °C, and 360 °C furnace temperature.

Statistics were calculated with IBM SPSS® 27, variables were tested for normal distribution with Shapiro-Wilk test, and means were compared by analysis of variance (ANOVA) with a post-hoc Scheffé test.

2.2 Thermal analysis experiments

Untreated beech and spruce wood and residues from the furnace experiments at 240 °C and 270 °C were milled with a Retsch Ultra Centrifugal Mill ZM 200 and sieved to particle sizes < 200 µm. Approx. 5 mg of the sieved material was weighed into an aluminium crucible and closed with a pierced lid. Simultaneous thermal analysis was conducted with a Netzsch STA 409 PG under oxidative conditions. The heating rate was 10 K min⁻¹ in the temperature range of 25 to 600 °C. Purge gas was air with a flow rate of 40 ml min⁻¹, and flushing gas for the scale was nitrogen with a flow rate of 60 ml min⁻¹.

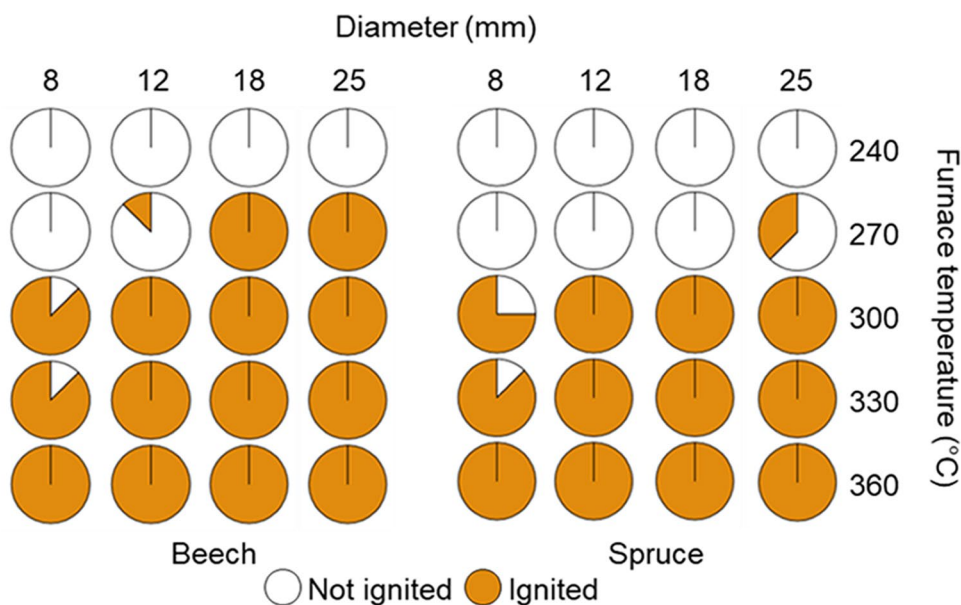
2.3 Proximate and ultimate analysis

Material for the proximate and ultimate analysis was milled with a Retsch Ultra Centrifugal Mill ZM 200 and sieved to particle sizes between 1000 and 200 µm. Moisture content was measured with a Kern DAB moisture analyser, CHN with Leco Truspec. Ash content was measured based on DIN EN 14775 and volatile matter based on DIN 51720:2001-03 and DIN EN 15148:2010-03. Calorific value was determined with an IKA C200 bomb calorimeter.

3 Results

The relation between furnace temperature (T_{furnace}), diameter of the spheres, wood species, and if an ignition happened or not is shown in Fig. 4. Ignition was determined by observation, whether the sphere was only pyrolyzed or burned completely after removal of the rack from the muffle furnace. Every circle in Fig. 4 represents the eight repetitions. For both species, the probability to ignite is growing with rising diameter and furnace temperature. At 240 °C, none of the specimens ignited, and no differences can be seen between beech and spruce. Starting at 270 °C, differences between the wood species appear, as all beech samples with a diameter bigger than 18 mm and one specimen with

Fig. 4 Ignited and not-ignited samples with 8, 12, 18, and 25 mm at the five used furnace temperatures, each circle represents 8 repetitions



12 mm, but only three of the spruce spheres with 25 mm ignited. The tendency for earlier ignition of beech wood continues at 300 °C but less pronounced, and seven beech specimens compared to six spruce specimens of the 8-mm spheres combusted. Differences between the number of ignited samples vanish completely at a furnace temperature of 330 °C. At a furnace temperature of 330 °C, only one 8-mm sphere did not ignite for both wood species, and at 360 °C, all specimens combusted.

Example curves from the furnace experiments can be seen in Figs. 5 and 6. For every furnace temperature, one sample curve for every diameter and wood species is shown. At higher furnace temperatures, the reaction speed generally tends to increase for all samples. Between 350 and 400 °C sample temperature, the heating rate decreases (visible as a change in the steepness of the curve) before taking up speed again. This decrease is visible at all furnace temperatures for both wood species, but more pronounced at furnace temperatures of 300 °C, 330 °C, and 360 °C.

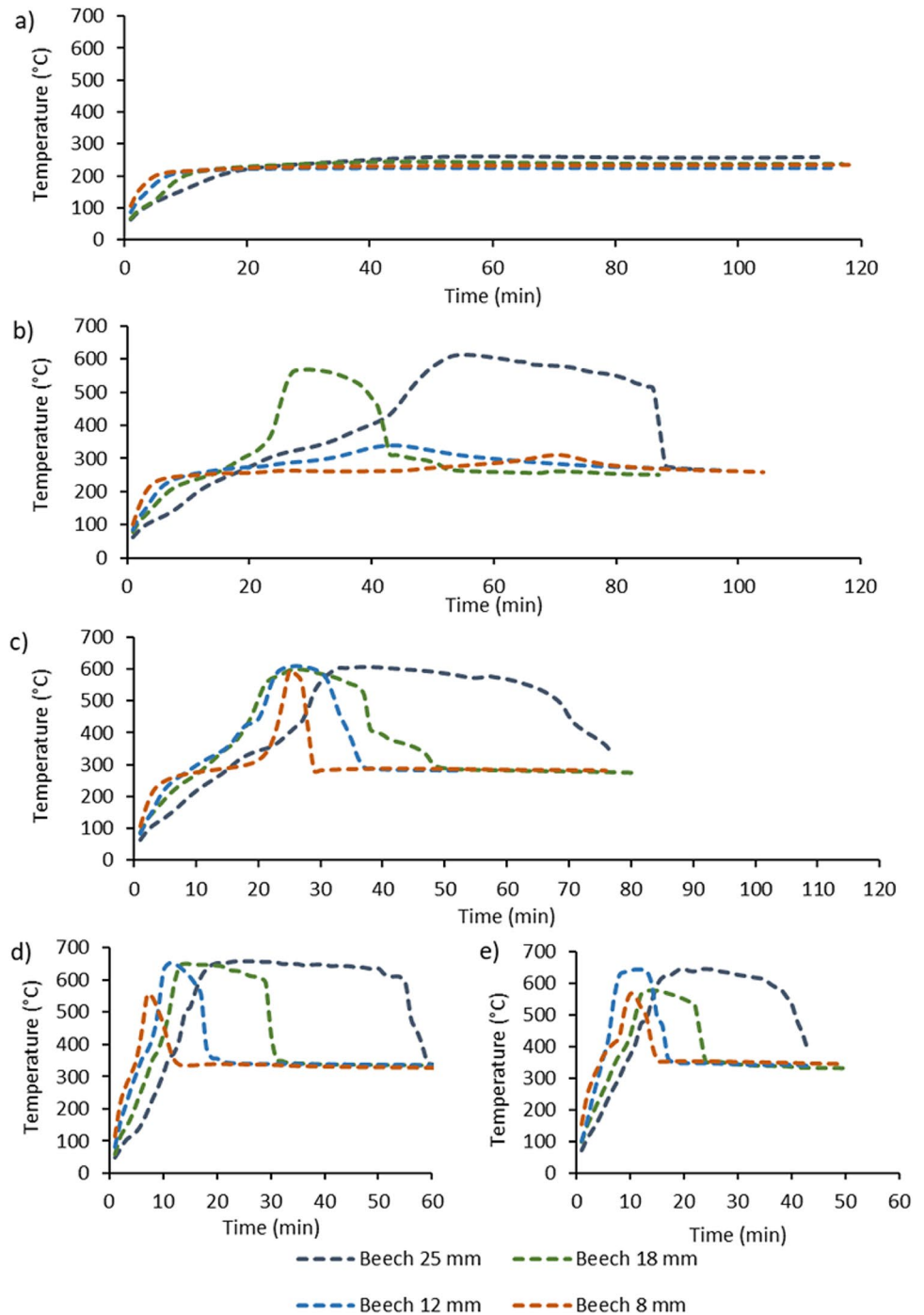
Ignition of the spheres happens in a glowing mode; this was observed for every temperature level except 240 °C, where no ignition happened at all. Table 2 shows the maximum temperatures that were measured between the 25- and 18-mm spheres and the 12- and 8-mm spheres.

Heating rate until the samples reached approx. furnace temperature is dependent on the furnace temperature and the dimension of the specimens (see Fig. 7). For all furnace temperatures, a clear trend for higher heating rates with smaller diameters is apparent. Heating rates for samples with the same diameter at the same furnace temperature are similar, with higher deviations for smaller diameters. In addition, an analysis of the Biot number (Bi) was performed to determine whether or not the temperature distributions inside the

spheres were the same and could be compared to each other [33]. The convective heat transfer coefficient under natural convection was calculated with an online tool provided by Tera Analysis Ltd. [34], and computed values for all spheres at all furnace temperatures are listed in Table 3. Values for the thermal conductivity were taken from Vay et al. [35]. For all samples, the calculated Biot numbers were similar in the range of 1 to 2.

An overview of all maximum temperatures (T max) measured with the thermocouples inside the spheres is presented in Fig. 8. At 240 °C, only the 25-mm beech samples showed a clear exothermic reaction, with core temperatures slightly above the furnace temperature. Differences between the species and the tested diameters start to increase at 270 °C, where the 18-mm and 25-mm beech samples already lit up and reached maximum temperatures of approx. 600 °C during combustion. For the spruce samples, the temperatures have a bigger distribution. In comparison with Fig. 4, it is apparent that some of the samples did not ignite, and therefore, maximum temperatures were lower. Nevertheless, all diameters except the 8-mm samples reached temperatures higher than furnace temperature, so exothermal reactions happened. Coming to 300 °C furnace temperature, the picture changes. On the one hand, all beech samples show clear exothermic reactions with T max of approx. 600 °C for all diameters, but on the other hand, differences between the 8 mm and the rest of the spruce samples are still visible, where temperatures stayed below 400 °C. At 330 °C and 360 °C furnace temperature, differences between the wood species disappear, although deviations are apparent, overall maximum temperatures where for most samples at approx. 600 °C.

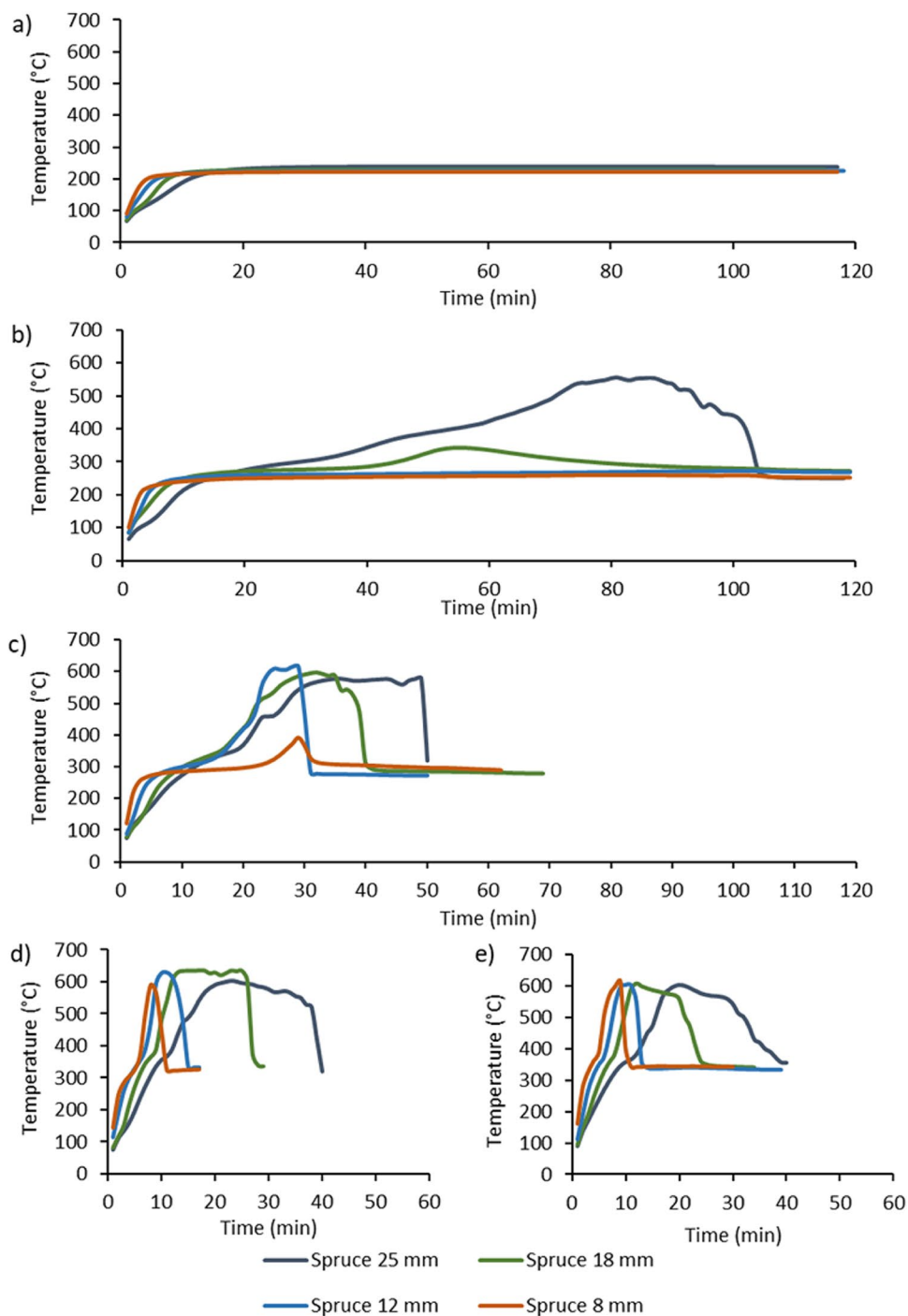
Fig. 5 Example temperature curves for beech samples with 25 mm, 15 mm, 12 mm, and 8 mm diameter at five different furnace temperatures: **a** 240 °C, **b** 270 °C, **c** 300 °C, **d** 330 °C, and **e** 360 °C



The duration of exothermicity is defined in this work as the time, when the temperature, measured inside the samples, was at least 20 °C higher than the furnace temperature. A diagram of the calculated values in seconds can be found in Fig. 9. Differences between the two wood species were apparent at all furnace temperatures. At 240 °C only, the 25-mm beech samples had in some cases measurable exothermal events, which lead to high deviations in the recorded data. Except the 8-mm samples, all

spheres made of beech showed exothermic reactions at 270 °C, and the longest duration was seen for the 25-mm samples. The 8-mm and 12-mm spruce samples showed no exothermal events at 270 °C furnace temperature. For 300 °C, 330 °C, and 360 °C, beech samples have a longer duration of exothermicity than samples made from spruce wood with the same diameter. Additionally, mean values and standard deviations of the three analysed variables and the mass loss in per cent can be found in Table 4.

Fig. 6 Example temperature curves for spruce samples with 25 mm, 15 mm, 12 mm, and 8 mm diameter at five different furnace temperatures: **a** 240 °C, **b** 270 °C, **c** 300 °C, **d** 330 °C, and **e** 360 °C



For the 8 mm diameter samples, a determination of the mass-loss was not possible, as the residues were too light.

Thermograms of the residues of beech and spruce samples at 240 °C can be found in Fig. 10. Moisture content (%) (determined as the lost mass at 120 °C), onset (°C), inflection (°C), and residual mass (%) of the measurements are listed in Table 5. Temperature measurements from the furnace experiments are reasonable, as the samples that reached a higher temperature reflect more of the characteristics of char coal.

Figure 10a shows differences between the 25-mm sphere and the other spheres, which were also slightly thermally modified, but fewer differences can be seen compared to the raw material (curve beech). Figure 10b delivers a different picture, as all the samples have almost the same onset temperature (approx. 300 °C), proving that the degree of oxidative pyrolysis is almost the same. In both cases, a shift of onset and inflection to higher temperatures is the cause of oxidative pyrolysis and a higher degree of thermal decomposition.

Table 2 Maximum temperatures measured during mode of ignition experiments between the 25 and the 18 mm and the 12 and 8 mm sphere at temperatures of 270 °C, 300 °C, 330 °C, and 360 °C

Position of TC	Furnace (°C)	Beech (°C)	Spruce (°C)
25 mm/18 mm	270	289.1	273.8
12 mm/08 mm	270	290.1	278.3
25 mm/18 mm	300	315.4	324.8
12 mm/08 mm	300	306.5	304.7
25 mm/18 mm	330	350.2	354.9
12 mm/08 mm	330	347.5	343.4
25 mm/18 mm	360	390.3	371.9
12 mm/08 mm	360	377.6	372.6

Figure 11a shows the thermograms of beech wood spheres in 270 °C furnace temperature. Since all beech samples with diameters of 25 mm and 18 mm combusted during the experiments (see Fig. 4 left), only the curves for 8 mm and 12 mm are shown. An even stronger shift to higher onset temperatures than in Fig. 10a can be seen as the maximum temperature of the spheres, and thus, the degree of oxidative pyrolysis rises. TG-measurements of the spruce leftovers show another picture. The 18-mm and 25-mm spheres already show a single step decomposition, which looks more like charcoal than wood, and the 8-mm and 12-mm samples still have the characteristics of thermally modified wood, as two consecutive decomposition steps can be seen. Differences between the largest beech and spruce spheres are almost non-existent.

4 Discussion

The tendency of spherical beech and spruce wood samples to ignite and subsequently combust is shown to be influenced by the wood species, the diameter, and the furnace

temperature. Ignition of the samples happens due to heterogeneous reactions on the pyrolyzed surface in combination with internal self-heating and subsequent combustion takes place in a glowing mode [1, 5]. This was observed in the mode of ignition experiments, where the closed door of the muffle furnace was switched out for a glass window. The arising maximum temperatures between the spheres (see Table 2) show a trend of higher heat emission at higher furnace temperatures. Heat emissions were present during glowing combustion of the spheres, but never reached temperatures higher than 30 °C above furnace temperature. As the thermocouples were located exactly between the spheres, approx. 10 mm away, an interaction of the combusting spheres can be excluded. Maximum arising temperatures inside the spheres of approx. 600 to 700 °C support this conclusion [3, 25]. First internal overheating in beech samples already happens at 240 °C furnace temperature (see Fig. 8). More severe exothermic ignition and combustion reactions were apparent at temperatures as low as 270 °C for beech samples with a diameter of 18 mm and 25 mm for all specimens and for one-third of the 25-mm spruce samples. With rising furnace temperatures, the differences in ignition propensity between the wood species and the diameter of the samples vanish more and more and are gone completely at

Table 3 Convective heat transfer coefficient for natural convection calculated

	Convective heat transfer coefficient ($\text{W m}^{-2}\text{K}^{-1}$) (calculated with [34])			
	8 mm	12 mm	18 mm	25 mm
240 °C	22.3	18.1	15.0	13.1
270 °C	22.8	18.6	15.4	13.4
300 °C	23.4	19.0	15.7	13.7
330 °C	23.8	19.3	16.0	13.9
360 °C	24.3	19.7	16.3	14.1

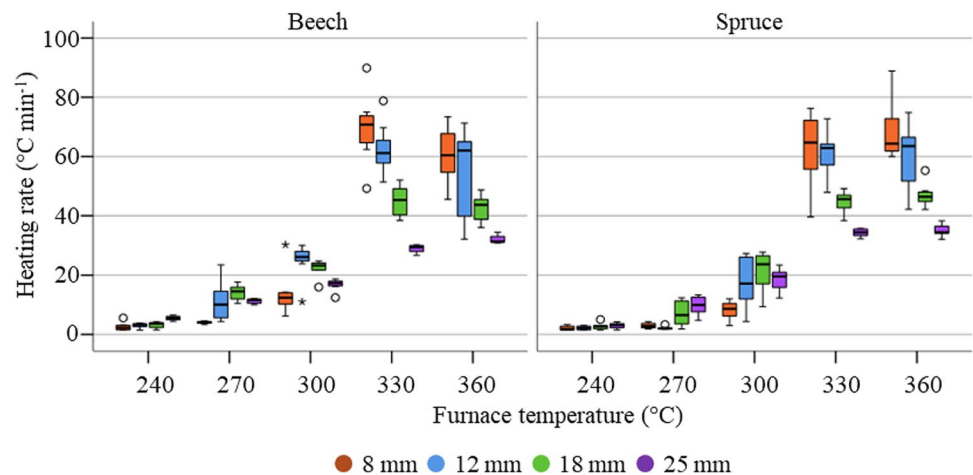
Fig. 7 Heating rate of beech and spruce samples at the five used furnace temperatures ($n = 8$)

Fig. 8 Maximum temperatures reached inside the beech and spruce wood spheres at the five used furnace temperatures ($n = 8$)

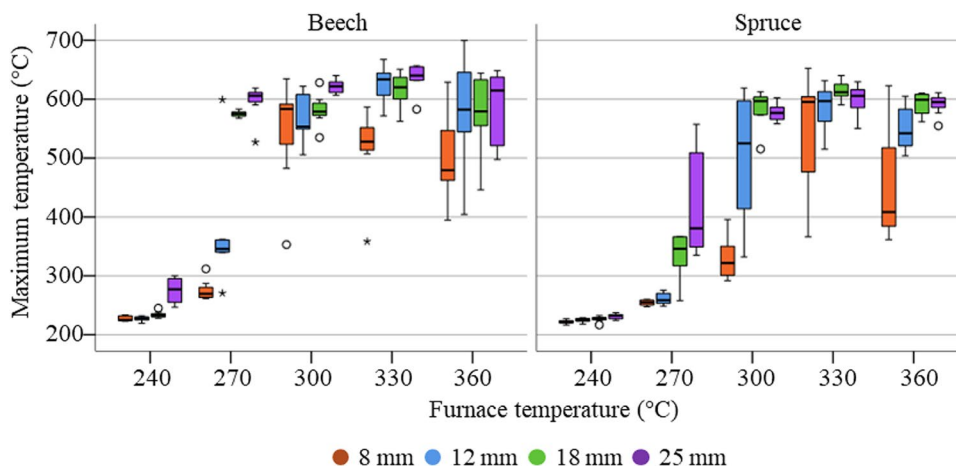
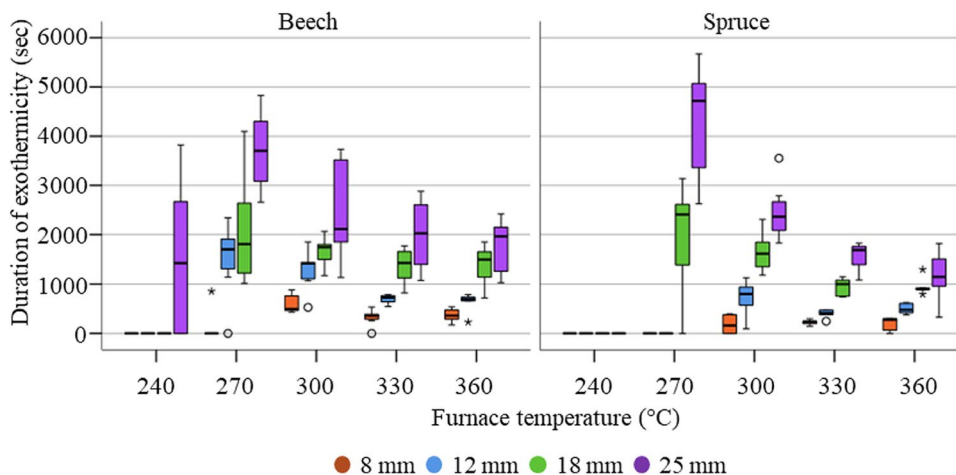


Fig. 9 Duration of exothermic reaction in minutes (time while temperature inside the spheres was higher than furnace temperature) for beech and spruce wood samples at the five used furnace temperatures ($n = 8$)



360 °C. For beech wood, the minimum temperature at which ignition and complete combustion is possible in the given time, and temperature range is between 240 and 270 °C for samples of a minimal diameter of 18 mm, and for spruce, the auto-ignition temperature is at approx. 270 °C for samples with a diameter of 25 mm. Especially at lower furnace temperatures, where chemistry has a greater influence on thermal decay than heat and mass transfer, the wood species itself strongly influences auto-ignition behaviour [36, 37]. Thermal events in the smaller samples tend to occur earlier than in larger samples. This may be due to the fact that more material takes longer to pyrolyze, and when ignition sets in, it takes longer for the temperature generated at the surface to reach the interior where the thermocouple is located, and similar findings were reported by Bennadji et al. [37].

The two used wood species differ in their physical properties and in their chemical composition [18, 32]. Until a temperature of 100 °C is reached inside the spheres, water evaporates from the samples. The evaporation enthalpy will lead to a delay of the pyrolysis process [1]. The first components of the wooden matrix to

decompose upon heating are the hemicelluloses, followed by cellulose and lignin [38]. Table 1 lists the chemical composition of the two wood species used according to Sjöström [32]. The majority of hemicelluloses in beech consists of xylan, which tend to decompose already at lower temperatures. This can be also seen in the thermograms shown in Figs. 10 and 11. In comparison to the mannan in spruce, xylan can show exothermal reactions even under pyrolytic conditions, which could be a cause for internal overheating of beech at lower temperatures [39]. The higher thermal stability of spruce might also be caused by more stable variants of cellulose and lignin in softwood species [40, 41]. Differences due to the physical properties can be seen in the heating rate (Fig. 7) until furnace temperature is reached inside the spheres. Thermocouple readings inside the smaller diameter samples (8 mm) are most likely influenced by the furnace temperature, to exhibit heating rates as high as 50 °C min⁻¹. For the larger samples, density is one influencing factor, as a higher density will result in lower heating rates under isothermal, pyrolytic conditions [42]. Calculated Biot

Table 4 Mean and standard deviation of the analysed variables heating rate ($^{\circ}\text{C}/\text{min}$); maximum temperature ($^{\circ}\text{C}$); duration of exothermicity (sec); and residual mass (%)

	Heating rate ($^{\circ}\text{C}/\text{min}$)			Maximum temperature ($^{\circ}\text{C}$)			Duration of exothermicity (sec)			Residual mass (%)		
Beech												
240 $^{\circ}\text{C}$												
8 mm	2.6	\pm	1.4	227.4	\pm	4.3	0.0	\pm	0.0	-	\pm	-
12 mm	3.1	\pm	0.8	227.3	\pm	4.2	0.0	\pm	0.0	60.8	\pm	38.0
18 mm	3.3	\pm	1.1	234.0	\pm	5.4	297.6	\pm	841.8	57.7	\pm	35.7
25 mm	5.5	\pm	0.7	275.3	\pm	21.6	4484.9	\pm	702.8	44.9	\pm	28.9
270 $^{\circ}\text{C}$												
8 mm	4.1	\pm	0.4	275.0	\pm	17.1	5047.3	\pm	818.7	-	\pm	-
12 mm	11.1	\pm	6.4	370.5	\pm	96.8	5092.4	\pm	806.0	41.4	\pm	9.1 ^a
18 mm	14.2	\pm	2.5	575.1	\pm	5.0	4949.6	\pm	757.5	0.0	\pm	0.0
25 mm	11.3	\pm	0.8	596.6	\pm	29.4	4662.0	\pm	759.1	0.0	\pm	0.0
300 $^{\circ}\text{C}$												
8 mm	13.1	\pm	7.5	511.7	\pm	125.5	3360.1	\pm	959.0	-	\pm	-
12 mm	22.8	\pm	8.1	578.4	\pm	44.7	3265.8	\pm	950.1	0.0	\pm	0.0
18 mm	20.8	\pm	4.9	547.7	\pm	100.6	3164.6	\pm	930.0	0.0	\pm	0.0
25 mm	16.8	\pm	2.0	621.5	\pm	11.4	2918.8	\pm	927.2	0.0	\pm	0.0
330 $^{\circ}\text{C}$												
8 mm	69.7	\pm	11.5	516.5	\pm	68.7	2736.9	\pm	1050.0	-	\pm	-
12 mm	62.4	\pm	8.4	626.2	\pm	30.2	3134.3	\pm	774.8	0.0	\pm	0.0
18 mm	45.0	\pm	5.2	616.2	\pm	29.0	3085.1	\pm	572.8	0.0	\pm	0.0
25 mm	29.0	\pm	1.3	636.9	\pm	24.1	3061.4	\pm	541.8	0.0	\pm	0.0
360 $^{\circ}\text{C}$												
8 mm	60.6	\pm	9.8	503.1	\pm	77.8	2596.7	\pm	293.0	-	\pm	-
12 mm	55.4	\pm	15.6	576.6	\pm	101.8	2491.3	\pm	248.2	0.0	\pm	0.0
18 mm	42.4	\pm	4.7	578.1	\pm	69.6	2464.6	\pm	285.2	0.0	\pm	0.0
25 mm	32.1	\pm	1.5	582.7	\pm	66.0	2354.1	\pm	262.0	0.0	\pm	0.0
Spruce												
240 $^{\circ}\text{C}$												
8 mm	2.1	\pm	0.7	222.0	\pm	3.2	0.0	\pm	0.0	-	\pm	-
12 mm	2.2	\pm	0.7	224.7	\pm	3.5	0.0	\pm	0.0	92.7	\pm	10.8
18 mm	2.7	\pm	1.1	226.7	\pm	4.7	0.0	\pm	0.0	89.0	\pm	3.4
25 mm	3.0	\pm	1.0	231.2	\pm	4.6	0.0	\pm	0.0	85.9	\pm	2.5
270 $^{\circ}\text{C}$												
8 mm	3.0	\pm	0.9	254.6	\pm	4.7	6084.0	\pm	775.1	-	\pm	-
12 mm	2.2	\pm	0.5	261.1	\pm	9.9	6137.1	\pm	916.7	67.1	\pm	10.3
18 mm	7.2	\pm	4.3	335.5	\pm	39.6	6045.9	\pm	866.6	44.1	\pm	12.2
25 mm	9.8	\pm	3.0	421.4	\pm	89.2	5984.4	\pm	701.5	31.3	\pm	12.6 ^b
300 $^{\circ}\text{C}$												
8 mm	8.2	\pm	3.1	329.2	\pm	35.2	3488.5	\pm	685.8	-	\pm	-
12 mm	17.8	\pm	8.4	503.1	\pm	108.0	3470.8	\pm	696.6	0.0	\pm	0.0
18 mm	21.5	\pm	6.8	584.6	\pm	31.3	3324.8	\pm	685.2	0.0	\pm	0.0
25 mm	18.6	\pm	3.7	577.3	\pm	15.0	3181.9	\pm	674.0	0.0	\pm	0.0
330 $^{\circ}\text{C}$												
8 mm	62.6	\pm	12.3	546.5	\pm	100.6	498.3	\pm	166.7	-	\pm	-
12 mm	61.1	\pm	7.6	586.5	\pm	37.6	644.1	\pm	137.3	0.0	\pm	0.0
18 mm	44.8	\pm	3.4	614.6	\pm	15.6	1306.6	\pm	51.1	0.0	\pm	0.0
25 mm	34.3	\pm	1.3	599.3	\pm	25.2	1759.5	\pm	298.3	0.0	\pm	0.0
360 $^{\circ}\text{C}$												
8 mm	68.9	\pm	10.6	456.8	\pm	112.9	2080.9	\pm	371.6	-	\pm	-
12 mm	59.6	\pm	11.5	551.4	\pm	39.0	2017.3	\pm	373.8	0.0	\pm	0.0
18 mm	47.1	\pm	4.2	591.4	\pm	20.0	1954.1	\pm	392.3	0.0	\pm	0.0
25 mm	35.1	\pm	2.1	591.2	\pm	19.2	1882.7	\pm	373.0	0.0	\pm	0.0

^aCalculated from 7 not burned samples^bCalculated from 5 not burned samples

Fig. 10 Thermograms of residues of beech (a) and spruce (b) samples at 240 °C furnace temperature. Maximum reached temperatures of the samples, according to measurements from furnace experiments, are added to the legend. Thermograms of raw beech and spruce are included as well

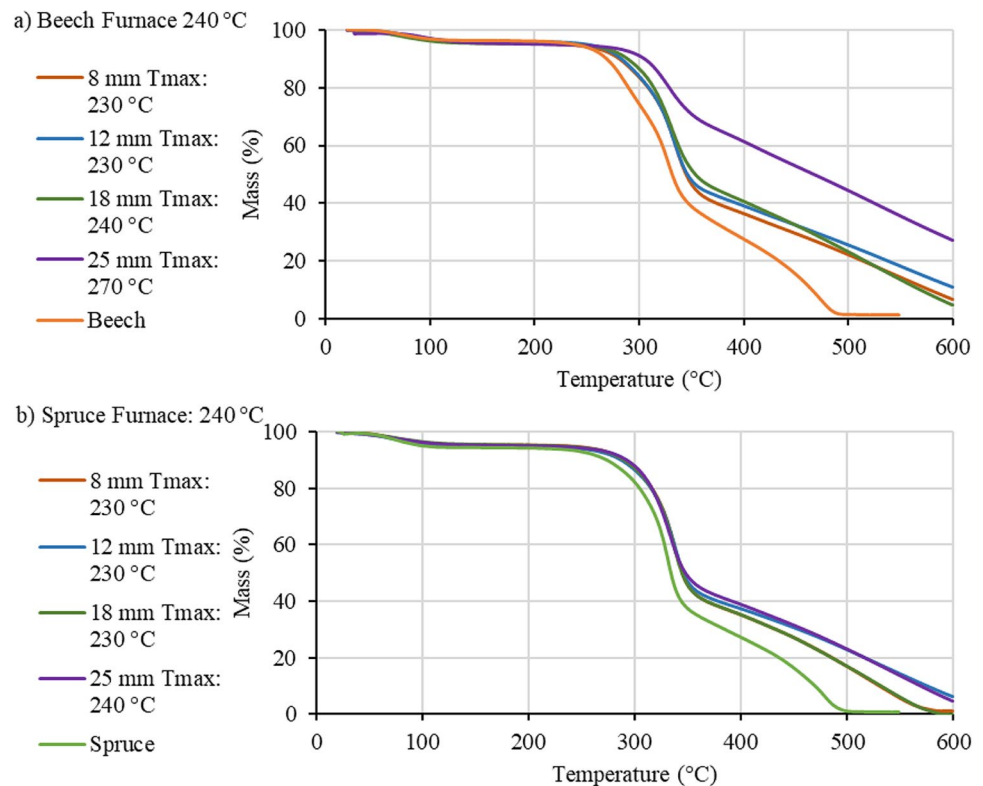


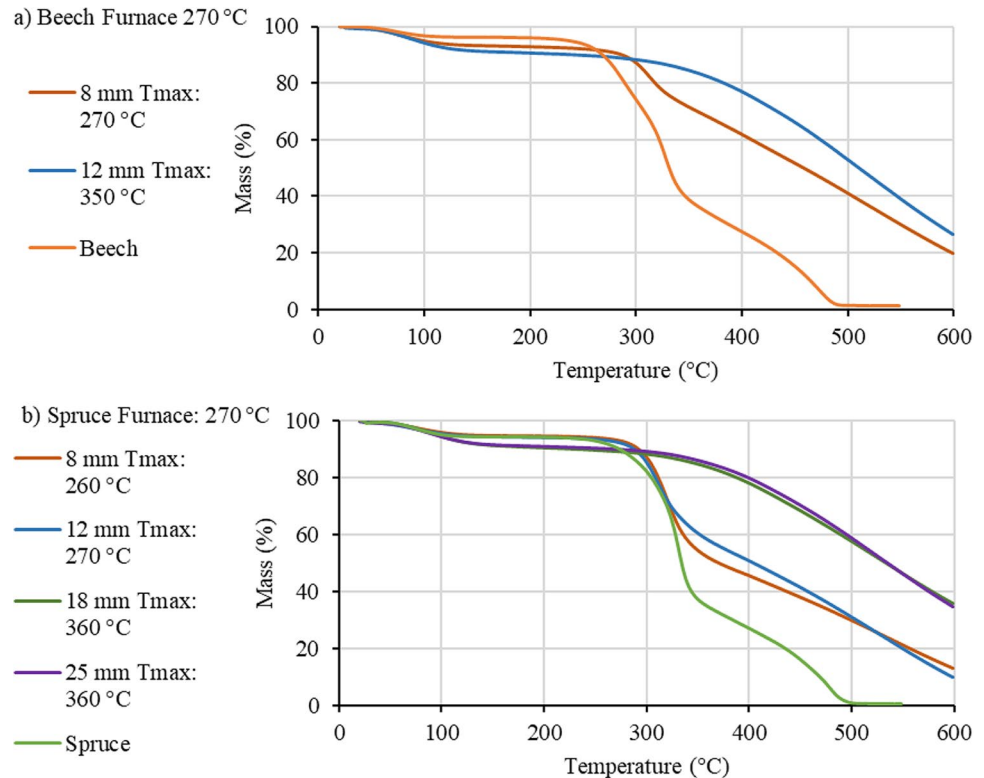
Table 5 TG data of the measured samples

Species	Diameter (mm)	Furnace temp (°C)	Moisture content (%)	Onset (°C)	Inflection (°C)	Residual mass (%)
Beech	-	-	3.7	263.1	329.1	1.4
Spruce	-	-	5.5	280.4	333.0	0.6
Beech	8	240	4.2	302.5	334.7	6.8
Beech	12	240	3.9	300.3	332.7	10.9
Beech	18	240	6.1	299.4	330.8	4.9
Beech	25	240	4.6	301.3	328.1	27.2
Spruce	8	240	5.1	300.6	338.1	1.3
Spruce	12	240	7.2	298.6	338.2	6.2
Spruce	18	240	7.0	301.0	337.0	0.0
Spruce	25	240	3.6	298.8	333.8	4.6
Beech	8	270	4.5	286.2	312.4	19.7
Beech	12	270	7.5	309.7	493.0	26.4
Spruce	8	270	4.2	293.2	319.8	13.2
Spruce	12	270	4.3	285.5	311.6	10.0
Spruce	18	270	4.7	303.5	537.3	35.6
Spruce	25	270	4.5	302.1	541.7	34.6

numbers for all samples were similar; therefore, the heating of the spheres is comparable [33]. Thermal expansion during pyrolysis, as described in Caposciutti et al. [43], and changing thermal conductivity during conversion to charcoal might also have an impact [44]. For 8 mm and 12 mm diameters, variations due to the furnace temperature influencing the temperature measured by the

thermocouples are possible. These problems could be the cause for high deviations in heating rate and maximum reached temperatures (Figs. 7 and 8, especially at 360 °C furnace temperature). Loss of contact between the thermocouples and the pyrolyzing and combusting samples might cause faulty measurements. During pyrolysis, the first increase in size of approx. 1–6% is followed by a

Fig. 11 Thermograms of residues of beech (a) and spruce (b) samples at 270 °C furnace temperature. Maximum reached temperatures of the samples, according to measurements from furnace experiments, are added to the legend. Thermograms of raw beech and spruce are included as well



severe shrinkage which leads to approx. 60–66% volume reduction [43]. Combining this two effects might cause cracking, and the rapid access of oxygen-rich air another causes for internal overheating and ignition [45]. During the heating of the samples, almost isothermal phases are visible between approx. 350 °C and approx. 400 °C, where heating slows down or no temperature change can be observed (see Figs. 5 and 6). It is suggested that these isotherms are caused by peak pyrolysis inside the wood samples, when all arising energy from exothermal reactions is used for the endothermal pyrolysis reactions [45]. Data from thermal analysis indicate that at 360 °C a shift in wood decomposition is happening. Depending on the atmosphere, severe endo- and exothermal reactions take place between 260 and 360 °C, due to devolatilization of hemicelluloses, cellulose, and lignin [22, 42]. The completion of the devolatilization step and the continuing oxidation of remaining char can be seen in the thermograms of raw beech and spruce wood and the only partially pyrolyzed samples in Figs. 10 and 11. Samples at 240 °C still have some characteristics of wood in the thermograms, which shows that the material is only partly pyrolyzed and still some hemicelluloses, cellulose, and lignin exist in their original or only slightly changed state [38]. Moisture content of the samples, determined as the mass lost until 120 °C, is present in all samples, as they are only partly pyrolyzed. Complete pyrolysis would have required at least 400 °C [46]. Nevertheless, the shift

of the onset to higher temperatures shows that some decomposition reactions took place, primarily hemicelluloses [40]. With rising heat treatment, temperature differences between the wood species disappear as the original composition is transformed into charcoal [46].

Similar plateaus were observed by various authors in oxidative and non-oxidative pyrolysis experiments [6, 47]. For ignition to happen, the material must reach at least 360 °C, and it does not matter whether this temperature is reached by external heating or by internal self-heating. This can be seen in Fig. 8, where temperatures of not-ignited samples did not surpass approx. 360 °C. While devolatilization due to oxidative pyrolysis is happening until 360 °C, a steady stream of volatiles pushes away the oxygen containing air from the highly reactive surface, so no heterogeneous reactions initiate further heating and decomposition of the pyrolyzed surface [1]. When reaching 360 °C, various changes in the wood structure occur under pyrolytic conditions, and precursors of charcoal might have a big impact, for example, by effecting the chemisorption behaviour [12, 46]. Pyrolytic conditions dominating in and around the samples during the heating period make the conducted experiments comparable to pyrolysis experiments [1]. As the experiments are performed in a well-ventilated combustion furnace, the lower flammability limit of pyrolysis gases in the surrounding air is not reached, so ignition and subsequent combustion happens in a glowing mode, as proven by the mode of ignition experiments [2].

5 Conclusions

The experiments used for the present study demonstrated the tremendous influence of isothermal temperature conditions on the auto-ignition of minimally different sized beech and spruce wood samples. Wood species and size of the sample influence the probability of auto-ignition. Beech samples tend to react already at lower temperatures than spruce samples, and larger samples ignite earlier than smaller ones. For beech samples with a diameter of 18 mm or bigger, the auto-ignition temperature is between 240 and 270 °C. Spruce samples with a diameter of 25 mm have an auto-ignition temperature of at least 270 °C. This difference can be explained by differences in the chemical structure of the hemicellulose, where beech wood mainly consists of xylan and spruce wood of mannan. During oxidative pyrolysis, the furnace temperature and the density of the wood species influence the heating rate. Denser species, such as beech, tend to heat more slowly, but ultimately have a longer exothermal reaction time. Isothermal phases at approx. 360 °C can be seen, while the samples are heated as the result of pyrolysis reactions of hemicellulose and cellulose, which absorb all the energy from the heterogeneous oxidation on the surface. Since the aim of the work was to study the auto-ignition process at ambient temperature and humidity, the samples were conditioned in the laboratory prior to the experiments. Future studies might include the influence on the moisture content on the auto-ignition properties.

Author contribution CPr and ASR contributed to the study conception and design. MW and CPr did all laboratory work and analysis of the data. CH and CPf were scientific advisors and supervisors for the whole process. The first draft was written by CPr. All authors contributed equally to final manuscript and approved.

Funding This work was supported by the Gesellschaft für Forschungsförderung Niederösterreich m.b.H. (GFF) and the government of Lower Austria (SC18-24). Open access funding is provided by the University of Natural Resources and Life Sciences Vienna (BOKU).

Data availability The data used to support the findings of this study are included in the article. Videos of the mode of ignition experiments can be shared if requested.

Declarations

Ethics approval This article does not contain any studies with human participants or animals performed by any of the authors.

Competing interests The authors declare no competing interests.

Open Access This article is licensed under a Creative Commons Attribution 4.0 International License, which permits use, sharing, adaptation, distribution and reproduction in any medium or format, as long as you give appropriate credit to the original author(s) and the source, provide a link to the Creative Commons licence, and indicate if changes were made. The images or other third party material in this article are included in the article's Creative Commons licence, unless indicated

otherwise in a credit line to the material. If material is not included in the article's Creative Commons licence and your intended use is not permitted by statutory regulation or exceeds the permitted use, you will need to obtain permission directly from the copyright holder. To view a copy of this licence, visit <http://creativecommons.org/licenses/by/4.0/>.

References

- Babrauskas V (2003) Ignition handbook: principles and applications to fire safety engineering, fire investigation, risk management and forensic science. Fire Science Publishers, Issaquah, Wash
- Jones JM, Saddawi A, Dooley B et al (2015) Low temperature ignition of biomass. *Fuel Processing Technology* 134:372–377. <https://doi.org/10.1016/j.fuproc.2015.02.019>
- Boonmee N, Quintiere JG (2005) Glowing ignition of wood: the onset of surface combustion. *Proc Combust Inst* 30:2303–2310. <https://doi.org/10.1016/j.proci.2004.07.022>
- Gray BF (2016) Spontaneous combustion and self-heating. In: Hurley MJ (ed) *SFPE Handbook of Fire Protection Engineering*, Fifth Edition. Springer, New York
- Babrauskas V (2002) Ignition of wood: a review of the state of the art. *J Fire Prot Eng* 12:163–189. <https://doi.org/10.1177/10423910260620482>
- Daouk E, van de Steene L, Paviet F et al (2014) Oxidative pyrolysis of a large wood particle: effects of oxygen concentration and of particle size. *Chem Eng Trans* 37:73–78. <https://doi.org/10.3303/CET1437013>
- Huang X, Rein G (2016) Thermochemical conversion of biomass in smouldering combustion across scales: The roles of heterogeneous kinetics, oxygen and transport phenomena. *Bioresour Technol* 207:409–421. <https://doi.org/10.1016/j.biortech.2016.01.027>
- Chen W-H, Lu K-M, Liu S-H et al (2013) Biomass torrefaction characteristics in inert and oxidative atmospheres at various superficial velocities. *Bioresour Technol* 146:152–160. <https://doi.org/10.1016/j.biortech.2013.07.064>
- Senneca O, Chirone R, Salatino P (2004) Oxidative pyrolysis of solid fuels. *J Anal Appl Pyrolysis* 71:959–970. <https://doi.org/10.1016/j.jaap.2003.12.006>
- Huang Y, Li B, Liu D et al (2020) Fundamental advances in biomass autothermal/oxidative pyrolysis: a review. *ACS Sustainable Chem Eng* 8:11888–11905. <https://doi.org/10.1021/acssuschemeng.0c04196>
- Rein G (2016) Smouldering combustion. In: Hurley MJ (ed) *SFPE Handbook of Fire Protection Engineering*, Fifth Edition. Springer, New York
- Bradbury AGW, Shafizadeh F (1980) Role of oxygen chemisorption in low-temperature ignition of cellulose. *Combust Flame* 37:85–89. [https://doi.org/10.1016/0010-2180\(80\)90073-5](https://doi.org/10.1016/0010-2180(80)90073-5)
- Lin S (2021) Fundamental study of near-limit smouldering fire dynamics. Hong Kong Polytechnic University
- Hagen BC, Meyer AK (2021) From smouldering to flaming fire: different modes of transition. *Fire Safety J* 121:103292. <https://doi.org/10.1016/j.firesaf.2021.103292>
- Anca-Couce A, Zobel N, Berger A et al (2012) Smouldering of pine wood: kinetics and reaction heats. *Combust Flame* 159:1708–1719. <https://doi.org/10.1016/j.combustflame.2011.11.015>
- Rupar-Gadd K, Forss J (2018) Self-heating properties of softwood samples investigated by using isothermal calorimetry. *Biomass and Bioenergy* 111:206–212. <https://doi.org/10.1016/j.biombioe.2017.04.008>
- Richter F, Atreya A, Kotsovinos P et al (2019) The effect of chemical composition on the charring of wood across scales. *Proc Combust Inst* 37:4053–4061. <https://doi.org/10.1016/j.proci.2018.06.080>

18. Wagenführ R (2000) Holzatlas, 5., erg. u.erw. Aufl. Fachbuchverl. im Hanser Verl., Leipzig
19. Mettler MS, Vlachos DG, Dauenhauer PJ (2012) Top ten fundamental challenges of biomass pyrolysis for biofuels. *Energy Environ Sci* 5:7797
20. Restuccia F, Mašek O, Hadden RM et al (2019) Quantifying self-heating ignition of biochar as a function of feedstock and the pyrolysis reactor temperature. *Fuel* 236:201–213. <https://doi.org/10.1016/j.fuel.2018.08.141>
21. Rebaque V, Ertesvåg IS, Mikalsen RF et al (2020) Experimental study of smouldering in wood pellets with and without air draft. *Fuel* 264:116806. <https://doi.org/10.1016/j.fuel.2019.116806>
22. Atreya A, Olszewski P, Chen Y et al (2017) The effect of size, shape and pyrolysis conditions on the thermal decomposition of wood particles and firebrands. *Int J Heat Mass Transfer* 107:319–328. <https://doi.org/10.1016/j.ijheatmasstransfer.2016.11.051>
23. Niemz P, Sonderegger W (eds) (2017) Holzphysik. Carl Hanser Verlag GmbH & Co, KG, München
24. Hurley MJ (ed) (2016) SFPE Handbook of Fire Protection Engineering, Fith. Springer, New York
25. Bilbao R, Mastral JF, Aldea ME et al (2001) Experimental and theoretical study of the ignition and smoldering of wood including convective effects. *Combust Flame* 126:1363–1372. [https://doi.org/10.1016/S0010-2180\(01\)00251-6](https://doi.org/10.1016/S0010-2180(01)00251-6)
26. Das S, Sarkar PK, Mahapatra S (2021) Single particle combustion studies of coal/biomass fuel mixtures. *Energy* 217:119329. <https://doi.org/10.1016/j.energy.2020.119329>
27. Martinka J, Mózer V, Hroncová E et al (2015) Influence of spruce wood form on ignition activation energy. *Wood Res* 60:815–822
28. Krigstin S, Helmeste C, Jia H et al (2019) Comparative analysis of bark and woodchip biomass piles for enhancing predictability of self-heating. *Fuel* 242:699–709. <https://doi.org/10.1016/j.fuel.2019.01.056>
29. Daouk E, van de Steene L, Paviet F et al (2015) Thick wood particle pyrolysis in an oxidative atmosphere. *Chem Eng Sci* 126:608–615. <https://doi.org/10.1016/j.ces.2015.01.017>
30. Miyawaki N, Fukushima T, Mizuno T et al. (2021) Effect of wood biomass components on self-heating. *Bioresour Bioprocess* 8. <https://doi.org/10.1186/s40643-021-00373-7>
31. Liu Q, Zhong Z, Wang S et al (2011) Interactions of biomass components during pyrolysis: a TG-FTIR study. *J Anal Appl Pyrolysis* 90:213–218. <https://doi.org/10.1016/j.jaap.2010.12.009>
32. Sjöström E (1993) Wood chemistry: fundamentals and applications, 2nd edn. Academic Press, San Diego
33. Baehr HD, Stephan K (2010) Wärme- und Stoffübertragung: Mit zahlreichen Tabellen sowie 62 Beispielen und 94 Aufgaben, 7., neu, bearb. Springer, Berlin, Heidelberg
34. Tera Analysis Ltd. (2023) Natural convection coefficient calculator --QuickField FEA software. https://quickfield.com/natural_convection.htm. Accessed 03 Feb 2023
35. Vay O, de Borst K, Hansmann C et al (2015) Thermal conductivity of wood at angles to the principal anatomical directions. *Wood Sci Technol* 49:577–589. <https://doi.org/10.1007/s00226-015-0716-x>
36. Di Blasi C, Branca C, Santoro A et al (2001) Pyrolytic behavior and products of some wood varieties. *Combust Flame* 124:165–177. [https://doi.org/10.1016/S0010-2180\(00\)00191-7](https://doi.org/10.1016/S0010-2180(00)00191-7)
37. Bennadji H, Smith K, Serapiglia MJ et al (2014) Effect of particle size on low-temperature pyrolysis of woody biomass. *Energy & Fuels* 28:7527–7537. <https://doi.org/10.1021/ef501869e>
38. Yang H, Yan R, Chen H et al (2007) Characteristics of hemicellulose, cellulose and lignin pyrolysis. *Fuel* 86:1781–1788. <https://doi.org/10.1016/j.fuel.2006.12.013>
39. Werner K, Pommer L, Broström M (2014) Thermal decomposition of hemicelluloses. *J Anal Appl Pyrolysis* 110:130–137. <https://doi.org/10.1016/j.jaap.2014.08.013>
40. Grønli MG, Várhegyi G, Di Blasi C (2002) Thermogravimetric analysis and devolatilization kinetics of wood. *Ind Eng Chem Res* 41:4201–4208. <https://doi.org/10.1021/ie0201157>
41. Awal A, Sain M (2011) Spectroscopic studies and evaluation of thermorheological properties of softwood and hardwood lignin. *J Appl Polym Sci* 122:956–963. <https://doi.org/10.1002/app.34211>
42. Di Blasi C, Branca C, Lombardi V et al (2013) Effects of particle size and density on the packed-bed pyrolysis of wood. *Energy & Fuels* 27:6781–6791. <https://doi.org/10.1021/ef401481j>
43. Caposciutti G, Almuina-Villar H, Dieguez-Alonso A et al (2019) Experimental investigation on biomass shrinking and swelling behaviour: particles pyrolysis and wood logs combustion. *Biomass and Bioenergy* 123:1–13. <https://doi.org/10.1016/j.biombioe.2019.01.044>
44. Hankalin V, Ahonen T (2009) Raiko R On thermal properties of a pyrolysing wood particle. *Finnish-Swedish Flame Days* 16:1–16
45. Park WC, Atreya A, Baum HR (2010) Experimental and theoretical investigation of heat and mass transfer processes during wood pyrolysis. *Combust Flame* 157:481–494. <https://doi.org/10.1016/j.combustflame.2009.10.006>
46. Tintner J, Preimesberger C, Pfeifer C et al (2018) Impact of pyrolysis temperature on charcoal characteristics. *Ind Eng Chem Res* 57:15613–15619. <https://doi.org/10.1021/acs.iecr.8b04094>
47. Bennadji H, Smith K, Shabangu S et al (2013) Low-temperature pyrolysis of woody biomass in the thermally thick regime. *Energy & Fuels* 27:1453–1459. <https://doi.org/10.1021/ef400079a>

Publisher's note Springer Nature remains neutral with regard to jurisdictional claims in published maps and institutional affiliations.